

Sound Diffuser Made of Acoustic Metamaterial: Numerical and Experimental Investigation

Jarosław RUBACHA

Corresponding author: Jarosław RUBACHA, email: jrubacha@agh.edu.pl

AGH University of Science and Technology, al. A. Mickiewicza 30, 30-059 Kraków, Poland

Abstract The use of metamaterials in room acoustics is becoming more and more popular. Their advantage is the possibility of adjusting the parameters of the systems in the desired frequency range and the reduction of dimensions compared to the existing solutions. This paper discusses the numerical design and experimental verification of sound diffuser based on the acoustic metamaterials: a slit with added quarter-wave length resonator. The transfer matrix method is used to make a numerical model of the metamaterial cell, which was used to build a model of a diffuser composed of $N = 7$ cells. Then, the dimensions of the diffuser were optimized to obtain the sound diffusion in a wide frequency range. The sound dispersion coefficient was also calculated using the FEM method. The numerical results were compared with the measurements and it was shown that it is possible to make a broadband sound diffuser with the use of metamaterials.

Keywords: metamaterial, sound diffusion, diffusion coefficient

1. Introduction

Sound diffusers are widely used in rooms requiring first reflection control, such as control rooms, recording studios, auditoriums, and concert halls. Contrary to sound-absorbing systems, diffusers enable the preservation of acoustic energy in the room. They ensure the even distribution of acoustic energy both in space and in time. The use of diffusers allows to eliminate of acoustic defects of the echo and reduce the coloration of the sound as a result of mirror reflections from hard surfaces [1]

Diffusers are specialized panels whose function is to scatter the reflected wave in many different directions. In the diffusers used so far, this is achieved through the use of a system of slots acting as quarter-wave resonators. The variation in the depth of the wells causes local delays of the phases of waves reflected from the bottom [2]. Designing the sound scattering is therefore the designation of an appropriate sequence of random numbers and the corresponding slit depths. The most commonly used is the QRD sequence. The lower frequency limit for sound scattering depends on the resonant frequency f_0 of the quarter-wave resonator $f_0 = c_0/4L$, where L is the probe depth and c_0 is the sound frequency in the air. In practice, this means that obtaining low-frequency diffusion requires the construction of large-thickness diffusers.

The use of acoustic metamaterials with spatial diffusers introduces strong dispersion. Such structures provide properties that are not found naturally in materials, such as negative effective bulk modulus, negative mass density [3], or slow-sound [4,5]. Taking advantage of the latter phenomenon enables to obtain maximum phase delay at low frequencies for relatively thin structures. There are known numerical analyses of diffusing systems based on metamaterial structures composed of slots loaded with Helmholtz resonators [6].

The research aimed to develop a sound diffuser made of cells of an acoustic metamaterial composed of slits loaded with a quarter-wave resonator. Such structure is characterized by strong dispersion and reduces the phase velocity c_p of the wave propagating in the material. This phenomenon is typical for metamaterials and provides a long delay of the phase of the reflected wave at lower frequencies. In consequence, it allows obtaining sound dispersion at lower frequencies compared to the classic QRD diffuser. A single metamaterial cell computational model using the transfer matrix method was developed and used in the $N=7$ cell diffuser model. The dimensions of the cells were then fine-tuned to obtain a diffusion of sound over a wide frequency range. A numerical model of the diffuser was also developed using

FEM to calculate the diffusion. The results of numerical calculations were compared with the measurements to verify the models.

2. Numerical model of the sound diffuser

2.1. Calculations of the sound diffusion coefficient

The quality of the sound dispersion by the surface characterizes the sound diffusion coefficient. It is determined for the angular distribution of the reflected sound pressure in the space above the diffuser. For a panel with a finite width of $2b$, the far-field angular pressure distribution $p_s(\theta)$ can be obtained from the Fraunhofer formula [2] (1):

$$p_s(\theta) = \int_{-b}^b R(x) e^{jk_0 x \sin\theta} dx, \quad (1)$$

where: θ – angular coordinate k_0 – wave number in the air, R – reflection coefficient.

Based on the reflection coefficient R , the diffusion coefficient d is calculated according to the formula (2):

$$d_\theta = \frac{(\sum |p_s(\theta)|)^2 - \sum |p_s(\theta)|^2}{(n-1) \sum |p_s(\theta)|^2}, \quad (2)$$

where: n – number of analyzed points in space above the diffuser.

To determine the diffusion coefficient of the structure, without the effect of scattering at the edge of the diffuser, the coefficient d_θ is normalized to the diffusion coefficient d_p for a flat plate with the same dimensions as the diffuser (3).

$$d_n = \frac{d_\theta - d_p}{1 - d_p}, \quad (3)$$

where: d_p – diffusion coefficient of the reference plate, d_θ – diffusion coefficient of the sound diffuser.

The values of the reflected sound pressure $p_s(\theta)$ from the diffuser were determined for the value of the reflection coefficient R , which was calculated using the Transition Matrix Method (TMM).

2.2. Metamaterial cell model - TMM

The sound diffuser is made of cells of metamaterials composed of slits loaded with quarter-wave resonators (see Fig. 1.).

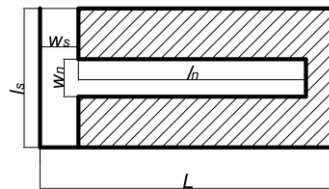


Fig. 1. Model of the metamaterial cell.

A theoretical model of a metamaterial cell was built using TMM [7–9]. The transition matrix \mathbf{T} combines the values of sound pressure p and the values of sound velocity v in front of the cell ($x = 0$) and behind the cell of the metamaterial.

$$\begin{bmatrix} p \\ v_x \end{bmatrix}_{x=0} = \mathbf{T} \begin{bmatrix} p \\ v_x \end{bmatrix}_{x=L} \quad (4)$$

It is assumed that only the plane wave propagates inside the cells. The reflection coefficient R is determined from the transmission matrix \mathbf{T} according to the formula:

$$R = \frac{T_{11} - Z_0 T_{21}}{T_{11} + Z_0 T_{21}}, \quad (5)$$

where: $Z_0 = \rho_0 c_0 / S_0$, $S_0 = Ll_s$.

Assuming that the resonator is a point diffuser placed in the middle of the main slit, the equivalent matrix for a single cell \mathbf{T}_k can be represented as:

$$\mathbf{T}_k = \mathbf{T}_m \mathbf{T}_p \mathbf{T}_m, \quad (6)$$

where \mathbf{T}_m – transmission matrix for half of the length of the main slit,

$$\mathbf{T}_m = \begin{bmatrix} \cos k_s \frac{l_s}{2} & iZ_s \sin k_s \frac{l_s}{2} \\ i/Z_s \sin k_s \frac{l_s}{2} & \cos k_s \frac{l_s}{2} \end{bmatrix}, \quad (7)$$

\mathbf{T}_p – transmission matrix for quadratic-wave length resonator,

$$\mathbf{T}_p = \begin{bmatrix} 1 & 0 \\ 1/Z_p & 1 \end{bmatrix}, \quad (8)$$

$$Z_p = -\frac{iZ_r \cot k_r l_r}{\phi_r}, \quad (9)$$

$Z_r = \sqrt{\kappa_r \rho_r}$ – the characteristic impedance of the quarter-wave-length resonator, $k_r = \omega \sqrt{\frac{\rho_r}{\kappa_r}}$ – the effective wave number in the slit of the resonator, $\phi_r = \frac{w_r}{l_s}$ – the porosity of the wall of main slit.

Thermo-viscous losses in the gaps were taken into account by using effective parameters:

$$\rho_{eff} = \rho_0 \left[1 - \frac{\tanh(rG_\rho)}{rG_\rho} \right]^{-1}, \quad (10)$$

$$\kappa_{eff} = \kappa_0 \left[1 + (\gamma - 1) \frac{\tanh(rG_\kappa)}{rG_\kappa} \right]^{-1}, \quad (11)$$

where: $G_\rho = \sqrt{i\omega\rho_0/\eta}$, r – half of the width of slits, respectively $w_s/2$ and $w_r/2$, $\gamma = 1,4$ – the specific heat ratio of air, $\eta = 1,813 \cdot 10^{-5} \left[\frac{\text{kg}}{\text{m}\cdot\text{s}} \right]$ – the dynamic viscosity, $P_r = 0,71$ – the Prandtl number, $\kappa_0 = \gamma P_0$ [Pa] – the air bulk modulus, $P_0 = 101325$ [Pa] – the atmospheric pressure, $\rho_0 = 1,21 \left[\frac{\text{kg}}{\text{m}^3} \right]$ – the air density.

2.3. Optimized sound diffuser

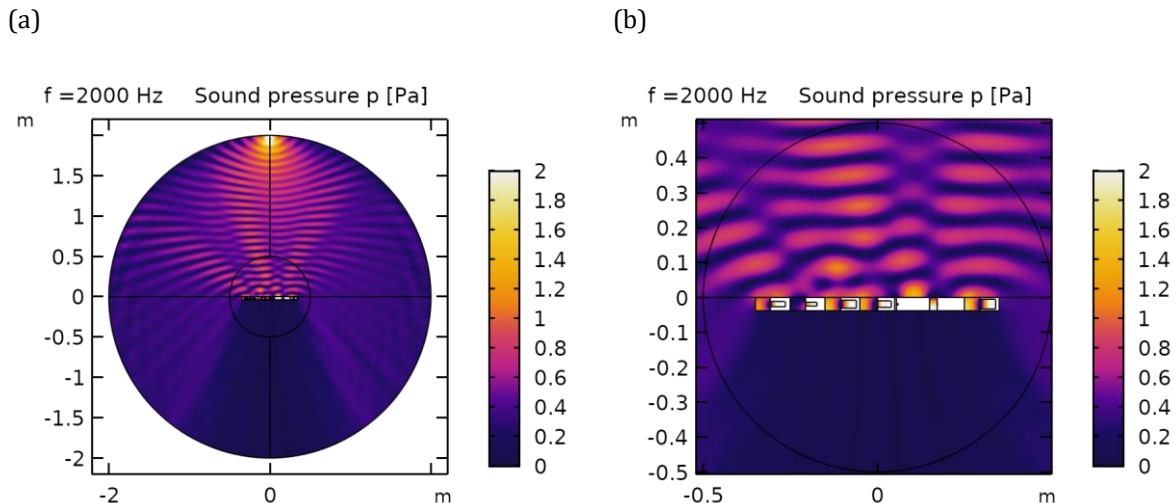
The dimensions of the diffuser have been optimized to obtain sound dispersion in a wide frequency range. The *fminimax* function from the Matlab tool was used for the calculations. It was assumed that the diffuser will consist of $N=7$ cells. Each cell was characterized by 3 parameters w_s , l_n , and w_n which were optimized. The remaining dimensions were assumed to be the same for all cells, ie cell width $L=100$ [mm] and the main slot length $l_s=38$ mm. For the optimization $f_0 = 1 - \bar{d}_{n(1000-4000)}$ was assumed as the objective function. The reflection coefficient R was calculated using the TMM model. As a result of the optimization, 21 dimensions characterizing the sound diffuser were determined (see Tab. 1.).

Tab. 1. Optimized dimensions of the sound diffuser

| Parameter | 1 | 2 | 3 | 4 | 5 | 6 | 7 |
|-----------|------|------|------|------|-----|------|------|
| N | 1 | 2 | 3 | 4 | 5 | 6 | 7 |
| ws [mm] | 43,0 | 44,0 | 45,0 | 51,0 | 5,0 | 22,0 | 45,0 |
| ls [mm] | | | | 38,0 | | | |
| wn [mm] | 15,0 | 11,0 | 25,0 | 19,0 | 5,0 | 5,0 | 28,0 |
| ln [mm] | 43,0 | 33,0 | 45,0 | 39,0 | 5,0 | 1,0 | 45,0 |

2.4 Numerical model of the sound diffuser - FEM

The FEM model was developed in COMSOL-Multiphysics. A 2D model was built, consisting of a circular main domain with a diameter of 4 m filled with air (Fig. 2a). In the middle of the domain was placed a one period of the sound diffuser consisting of $N=7$ cells (Fig. 2b). The diffuser boundary was rigid. In narrow cell slits, thermo-viscous losses were taken into account. At the outer edge of the main domain, the boundary condition of radiating a cylindrical wave was adopted to ensure free field conditions. The sound pressure values for the reflected wave $p_s(\theta)$ were calculated for distance $r=2$ m for the diffuser and the reflective surface, respectively. Then, according to the formulas (2 and 3), the diffusion coefficients d_θ and d_p and d_n were determined.

**Fig. 2.** Model of the metamaterial cell.

3. Verification of the numerical models

The results of numerical calculations were verified by comparing the numerically calculated values in the TMM and FEM models with the measurement results. The calculations were performed for optimized dimensions of the diffuser (Tab.1.)

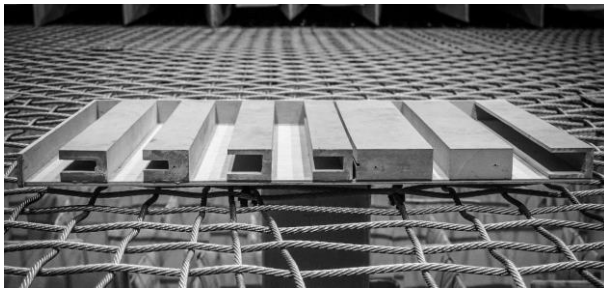
3.1. Measurement of the diffusion coefficient

For the optimized dimensions, a physical model (Fig. 3a) of the sound diffuser was made. The model made of MDF board had dimensions of 700x450x38 mm. Measurements of the diffusion coefficient were carried out on a measuring stand in an anechoic chamber (Fig.3b) according to ISO 14793-1 [10].

The measuring stand consisted of a sound source placed above the sample at a height of 4 m. The recording of the acoustic pressure reflected from the tested surface was carried out on an arc with a radius of 2 m above the sample with an angular resolution of 5°. The microphone was moved using a gauge manipulator. The values of the sound pressure reflected from the tested surface for a given angle $p_s(\theta)$ were determined by the subtraction method. The impulse responses of the empty station were subtracted from the impulse

responses tested for the sample and the flat surface. This eliminated the impulse responses; direct sound and unwanted reflections from the elements of the test stand. As a result, there remained fragments of impulse responses containing, respectively, reflections from the tested sample and the flat surface. The signal was then filtered in 1/3 octave bands and the $p_s(\theta)$ values were calculated. Then, according to the formulas (2 and 3), the diffusion coefficients d_θ and d_p and d_n were determined. The measurement uncertainty of type B was estimated according to the method described by Pilch[11].

(a)



(b)

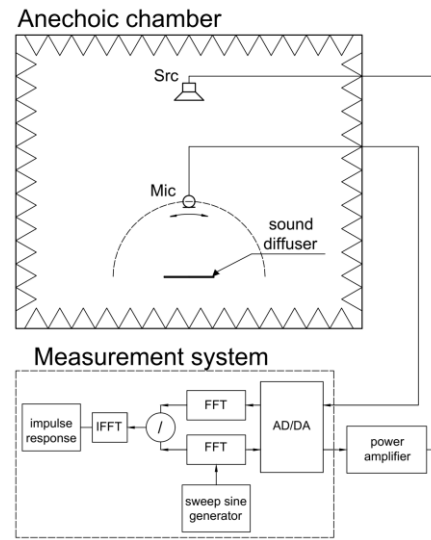


Fig. 3. a) Sound diffuser composed of metamaterial and b) stand for measuring the diffusion coefficient in the anechoic chamber.

3.2 Discussion

The analysis of the reflectance phase delay calculated in TTM model showed that in the frequency range 1-2 kHz, the phases of reflection coefficient $\arg R/\pi$ from individual cells are the most diverse (Fig. 4). This coincides with the range in which the sound diffusion coefficient d_n has the highest values (Fig 5d). Moreover, the applied cells of the acoustic metamaterial cause a reduction of the phase velocity c_p , of the sound propagating in the structure. This ensures a longer delay of the wave reflected from the structure for lower frequencies than in classic QRD diffusers. This can be seen for cells 1 and 7 for which the delays are the longest (Fig. 4). In contrast, for cells 5 and 6, which are slots without resonators, the delays are the smallest. As a result, the applied metamaterial structure allows obtaining a full period phase delay for frequencies about 1000 Hz lower than in classic QRD diffusers.

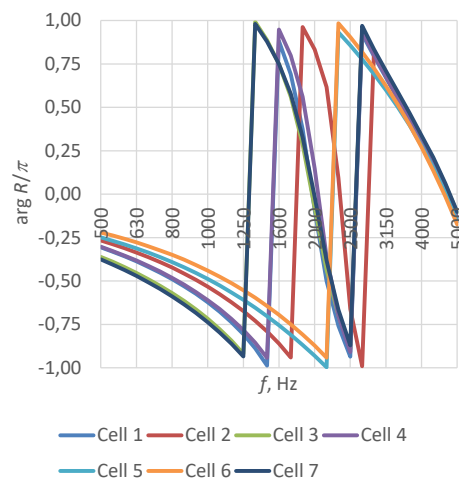


Fig. 4. Phase of the reflection coefficient for each cell.

The model verification showed that the measured and calculated in the FEM model values of the normalized reflected sound pressure level $L_{ps}(\theta)$ from the diffuser show a high agreement. As a result, the diffusion coefficients also assume similar values (Fig.5a,b,c). The significant difference of the L_{ps} values between the measurement and calculated in the TMM model occurs for high reflection angles at the frequency of 2000 Hz. Calculated values of L_{ps} are higher (over 10dB), and consequently, the diffusion coefficient values are higher (Fig.5b,c). On the other hand, the angular distribution of the side lobes for the TMM model and the measurement is convergent. This proves that the phase shifts in the TMM model were correctly determined. The L_{ps} values may vary because the calculations in the TMM model were performed for $r \rightarrow \infty$, while measurement and calculation in the FEM model were performed in distance $r=2$ m. The TMM model also does not take into account the interaction between cells. Calculation of the reflection coefficient R was performed for each cell separately, and then the $p_s(\theta)$ was calculated from the Fraunhofer integral for the $N=7$ cells. On the other hand, the FEM model takes into account the full geometry of the diffuser, so the calculation takes into account the interaction between the cells. The values of the normalized sound diffusion coefficient d_n calculated in the FEM model are consistent. For most frequency bands, the differences are within the measurement uncertainty (Fig.5d). Values calculated in the TMM model are overestimated, however, the frequency range in which the diffusion occurs is similar.

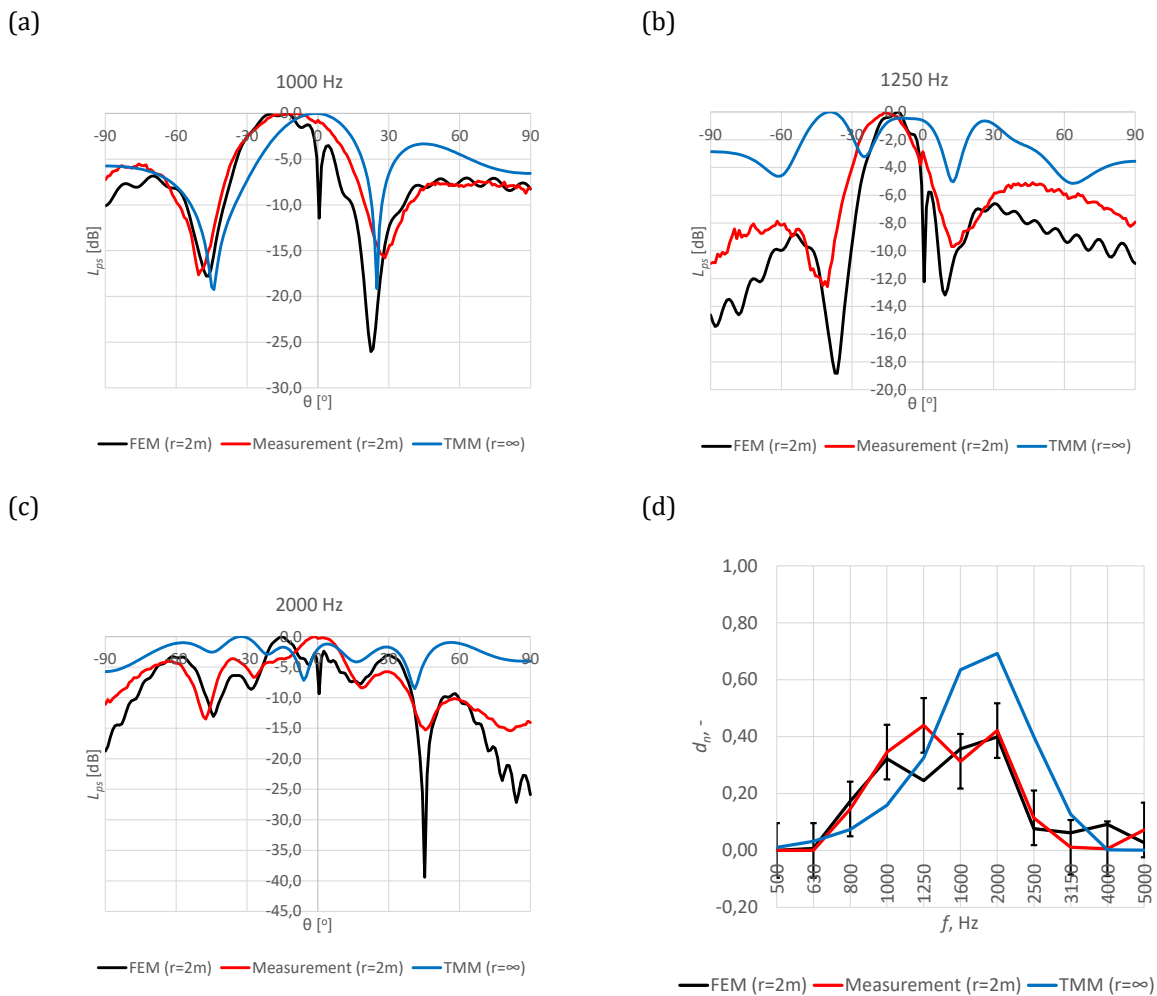


Fig. 5. Reflected sound pressure level L_{ps} in frequencies: a) 1000 Hz, b) 1250 Hz and b) 2000 Hz. d) Comparison of the numerically calculated and measured values of the normalized diffusion coefficient.

4. Conclusions

The article presents a sound diffuser composed of acoustic metamaterials. A computational model for determining the sound diffusion coefficient using the transition matrix method was used to optimize the diffuser to broaden the frequency range. Used optimal dimensions, the physical model of the diffuser was made and measurements were carried out. A numerical model of the diffuser was also made using the FEM method. The measurement results were used to verify the TMM and FEM numerical models. The analysis of the results showed that effective scattering by optimized sound diffuser occurs in the frequency range 1000-2000 Hz. Verification shows also that the determined frequency range in which the diffuser will diffuse the sound is consistent with measurement and the FEM model. However, not taking into account the interaction of cells in the TMM model may significantly affect the determined values of the sound dispersion coefficient. The calculation of the sound dispersion coefficient using the TMM model allows for a fast calculation of the diffusion coefficient. The FEM model of the whole diffuser allows to obtain more accurate calculation results, however, it is time-consuming and significantly extends the calculation time of the optimization process.

References

1. T.J. Cox, P. D'Antonio. : Acoustic Absorbers and Diffusers Theory, Design and Application. CRC Press, 2017.
2. T.J. Cox, P. D'Antonio. Acoustic phase gratings for reduced specular reflection. *Applied Acoustics*, 60(2):167–186, 2000.
3. Y. Ding, Z. Liu, C. Qiu, J. Shi. Metamaterial with Simultaneously Negative Bulk Modulus and Mass Density. *Physical Review Letters*, 99:093904, 2007.
4. J.P. Groby, W. Huang, A. Lardeau, Y. Aurégan. The use of slow waves to design simple sound absorbing materials. *Journal of Applied Physics*, 117:124903, 2015.
5. J-P. Groby, R. Pommier, Y. Aurégan. Use of slow sound to design perfect and broadband passive sound absorbing materials. *The Journal of the Acoustical Society of America*, 139(4):1660, 2016.
6. doi: 10.1121/1.4945101.
7. N. Jiménez, T.J. Cox, V. Romero-García, J.P. Groby. Metadiffusers: Deep-subwavelength sound diffusers. *Scientific Reports*, 7:5389, 2017.
8. N. Jiménez, V. Romero-García, V. Pagneux, J.-P. Groby. Quasiperfect absorption by subwavelength acoustic panels in transmission using accumulation of resonances due to slow sound. *Physical Review B*, 95:014205, 2017.
9. N. Jiménez, W. Huang, V. Romero-García, V. Pagneux, J.-P. Groby. Ultra-thin metamaterial for perfect and quasi-omnidirectional sound absorption. *Applied Physics Letters*, 109:121902, 2016.
10. M.L. Munjal. *Acoustics of Ducts and Mufflers*. Wiley, Chichester, 2014.
11. ISO 17497-2 2012 Acoustics. Sound-scattering properties of surfaces. Part 2 Measurement of the directional diffusion coefficient in a free field. 2012.
12. A. Pilch. Sources of measurement uncertainty in determination of the directional diffusion coefficient value. *Applied Acoustics*, 129:268-276,2018.

© 2021 by the Authors. Licensee Poznan University of Technology (Poznan, Poland). This article is an open access article distributed under the terms and conditions of the Creative Commons Attribution (CC BY) license (<http://creativecommons.org/licenses/by/4.0/>).